CAVENDISH-HEP-99-15

Mass Effects in Bose-Einstein Correlations

Mark Smith
University of Cambridge, Cavendish Laboratory,
Madingley Road, Cambridge, England, CB3 0HE
(December 7, 1999)

Abstract

Bose-Einstein symmetrization can lead to correlations between out going identical particles which reflect the space-time extent of the collision process. At LEP and LEPII these correlations have been studied as a function of the single variable $Q = \sqrt{-(p_1 - p_2)^2}$. Assuming a simple form for the correlation function the experiments find source radii dependent on the hadron mass. In this note, I point out that such effects can arise from purely kinematic considerations, although these are unlikely to explain the observed effects completely.

I. INTRODUCTION

Bose-Einstein correlations are of interest to the LEP community as a source of systematic error in W-mass determinations (for example [1–4]), and also to the Heavy Ion community (see [5,6]) as a valuable measurement tool for the size of the fireball created in heavy ion collisions (eg. [7] and refs therein).

Due to limited statistics, measurements of BE enhancement at LEP are often made in terms of a single variable $Q = \sqrt{-(p_1 - p_2)^2}$ where p_1 and p_2 are the 4-momenta of a pair of out going bosons. The enhancement is described by a correlation function which introduces an extra parameter, the HBT (Hanbury-Brown-Twiss [8]) radius. It has been observed [9] that the radii measured depend on the mass of the boson being used. In general the lighter bosons tend to give larger radii. In this section I describe the construction of the correlation function as a function of Q and its relation to the single particle Wigner distribution. In section 2 I use a simple Gaussian model for the Wigner density, and discuss the correlation function in various limits. In section 3 numerical results are presented for particles of various different masses and sources of different sizes. I conclude with a discussion of how far these results can go to explain the observed mass dependence of experimental Bose-Einstein parameters.

The *correlation function* can be defined as

$$C(Q) = \frac{\rho_2(Q)}{\rho_1(Q)}, \tag{1.1}$$

where $\rho_2(Q)$ is the density of particle pairs with invariant momentum separation Q, and $\rho_1(Q)$ is the same density measured with respect to a reference distribution. The densities ρ_1 and ρ_2 can be defined in terms of the single- and two-particle momentum densities (P_1 and P_2 respectively) according to

$$\rho_1(Q) = \int d^3\mathbf{p}_1 \, d^3\mathbf{p}_2 \; P_1(\mathbf{p}_1)P_1(\mathbf{p}_2)\delta(\tilde{Q}(\mathbf{p}_1,\mathbf{p}_2) - Q) \tag{1.2}$$

$$\rho_2(Q) = \int d^3\mathbf{p}_1 \, d^3\mathbf{p}_2 \; P_2(\mathbf{p}_1,\mathbf{p}_2)\delta(\tilde{Q}(\mathbf{p}_1,\mathbf{p}_2) - Q), \tag{1.3}$$

where the function $\tilde{Q}(\mathbf{p}_1,\mathbf{p}_2)$ is just $\sqrt{-(p_1-p_2)^2}$.

The single-particle momentum distribution is given in terms of the one-particle Wigner distribution $S(x,p)$,

$$P_1(\mathbf{p}_1) = \int d^4x \; S(x,p)|_{p^2=m^2}. \tag{1.4}$$

It has long been known that under rather general assumptions the two-particle distribution can also be related to the one-particle Wigner density [10]

$$P_2(\mathbf{p}_1,\mathbf{p}_2) = P_1(\mathbf{p}_1)P_1(\mathbf{p}_2) + \left| \int d^4x \; S(x,K)e^{-iq\cdot x} \right|^2, \tag{1.5}$$

where $K = \frac{1}{2}(p_1+p_2)$ and $q = p_1 - p_2$. It is thus possible, given the source distribution, to compute the densities P_1 and P_2 and hence ρ_1 and ρ_2, then to construct explicitly the correlation function $C(Q)$. The correlation function $C(Q)$ may depend on the particle masses through the integration limits in equations (1.2) and (1.3), even when there is no explicit mass dependence in the source function S. In the next section I examine this implicit dependence for a Gaussian source.

II. SIMPLE MODEL

To illustrate the kinematical mass effects it is best to take a simple model. Consider an instantaneous, uncorrelated source, Gaussian in both space and momentum. The normalised source distribution is given by

$$\begin{aligned} S(x,p) = & \frac{1}{(2\pi R_0^2)^{\frac{3}{2}}} \exp\left(-\frac{|\mathbf{x}|^2}{2R_0^2}\right) \times \\ & \frac{1}{(2\pi P_0^2)^{\frac{3}{2}}} \exp\left(-\frac{|\mathbf{p}|^2}{2P_0^2}\right) \delta(x^0). \end{aligned} \tag{2.1}$$

The parameters R_0 and P_0 are the typical size of the source in position and momentum space, respectively. The single and two particle distributions can now be obtained using the formulae of the previous section:

$$P_1(\mathbf{p}) = \frac{1}{(2\pi P_0^2)^{\frac{3}{2}}} \exp\left(-\frac{|\mathbf{p}|^2}{2P_0^2}\right) \tag{2.2}$$

$$P_2(\mathbf{p}_1, \mathbf{p}_2) = P_1(\mathbf{p}_1)P_1(\mathbf{p}_2) + \frac{1}{(2\pi P_0^2)^3} \exp\left(-\frac{|\mathbf{K}|^2}{4P_0^2} - R_0^2|\mathbf{q}|^2\right), \tag{2.3}$$

where $\mathbf{K} = \frac{1}{2}(\mathbf{p}_1 + \mathbf{p}_2)$ and $\mathbf{q} = (\mathbf{p}_1 - \mathbf{p}_2)$. Note that in this simple example the fully differential particle distributions do **not** depend on the particle masses.

Inserting Eqs. (2.2,2.3) into Eqs. (1.2,1.3) and then constructing Eq. (1.1) gives the expression for the correlation function

$$C(Q) = 1 + \frac{\int d^3\mathbf{p}_1\, d^3\mathbf{p}_2\, \exp\left(-\frac{|\mathbf{p}_1+\mathbf{p}_2|^2}{4P_0^2} - R_0^2|\mathbf{p}_1 - \mathbf{p}_2|^2\right) \delta(\tilde{Q}(\mathbf{p}_1, \mathbf{p}_2) - Q)}{\int d^3\mathbf{p}_1\, d^3\mathbf{p}_2\, \exp\left(-\frac{|\mathbf{p}_1|^2}{2P_0^2}\right) \exp\left(-\frac{|\mathbf{p}_2|^2}{2P_0^2}\right) \delta(\tilde{Q}(\mathbf{p}_1, \mathbf{p}_2) - Q)}. \tag{2.4}$$

Due to the spherical symmetry of the source most of the angular integrations are trivial. The δ-function constraint can be satisfied with the angle between $\mathbf{p}_1$ and $\mathbf{p}_2$; define the cosine of this angle to be x. The integrations may then be re-written,

$$d^3\mathbf{p}_1\, d^3\mathbf{p}_2 \delta(\tilde{Q}(\mathbf{p}_1, \mathbf{p}_2) - Q) \longrightarrow p_1\, dp_1\, p_2\, dp_2 \Theta(1-x)\Theta(1+x) \tag{2.5}$$

where $p_i = |\mathbf{p}_i|, \quad i = 1, 2$. Constants independent of p_1 and p_2 have been dropped as these cancel in the ratio (2.4). The variable x as a function of p_1 and p_2 is given by

$$x = \left(\frac{\sqrt{(p_1^2 + m^2)(p_2^2 + m^2)} - m^2}{p_1 p_2}\right) - \frac{Q^2}{2p_1 p_2}, \tag{2.6}$$

where $\Theta(z)$ is the Heaviside (theta) function. Notice that mass dependence has now crept into $C(Q)$ via the integration limits.

The theta-functions in Eq. (2.5) give rise to a complicated integration region in the $p_1 - p_2$ plane which depends on the mass of the bosons. The integration region can be summarized as

$$p_2 > \left| p_1\left(1 + \frac{Q^2}{2m^2}\right) - Q\sqrt{\left(1 + \frac{p_1^2}{m^2}\right)\left(1 + \frac{Q^2}{4m^2}\right)}\right|, \tag{2.7}$$

$$p_2 < p_1\left(1 + \frac{Q^2}{2m^2}\right) + Q\sqrt{\left(1 + \frac{p_1^2}{m^2}\right)\left(1 + \frac{Q^2}{4m^2}\right)}. \tag{2.8}$$

This takes on simple forms in the following limits

$$\frac{Q}{m} \longrightarrow \infty : \quad p_2 > \frac{Q^2}{4p_1} \qquad \text{(the massless limit)} \tag{2.9}$$

$$\frac{Q}{m} \longrightarrow 0 : \quad p_1\left(1 - \frac{Q}{m}\right) < p_2 < p_1\left(1 + \frac{Q}{m}\right) \quad \text{where } p_1, p_2 \gg m. \tag{2.10}$$

$$\frac{Q}{m} \longrightarrow 0 : \quad |p_1 - Q| < p_2 < p_1 + Q \quad \text{where } p_1, p_2 \ll m \tag{2.11}$$

Now the BE enhanced region of the $p_1 - p_2$ plane lies on a band of thickness $\sim R_0^{-1}$ centered around $p_1 \approx p_2$, while the reference density lies largely in the region $p_1, p_2 \leq \mathcal{O}(P_0)$. Figures 1 and 2 show the enhanced region and the integration bounds for $Q < m$ and $Q > m$. It is then clear that for any $Q \gg m$ the enhanced region occupies a fraction $\mathcal{O}([R_0 P_0]^{-1})$ of the populated region. This factor must always be less than one by the uncertainty principle and so the strength of the correlation is reduced. In fact it is possible to show that in the massless limit, the intercept of the correlation function at $Q = 0$ occurs at

$$\begin{aligned} C(Q \approx 0) &= 1 + \left(\frac{\xi - (1 - \xi^2) \tan^{-1}(\xi)}{\xi^3} \right) \\ &\approx 1 + \frac{\pi}{2\xi} \quad \text{as } \xi \longrightarrow \infty, \end{aligned} \tag{2.12}$$

where $\xi = 2R_0 P_0$.

The opposite limit $Q \ll m$ is qualitatively different. One can see from Eq. (2.10) that as $Q \longrightarrow 0$ with $Q \ll m$, the integration region is squeezed into a narrow wedge along the diagonal of the $p_1 - p_2$ plane (the integration region in figure 1 is approaching this limit). If the inequality

$$\frac{P_0 Q}{m} < \frac{1}{R_0} \qquad \Longleftrightarrow \qquad Q < \frac{m}{R_0 P_0} \tag{2.13}$$

is satisfied then the integration region only contains the enhanced region and the correlation function can approach the expected value of $C(Q \approx 0) = 2$. In fact in the limit that the mass is large compared to all other scales, the correlation function approaches the 'naive' form

$$C(Q) = 1 + \exp(-Q^2 R_{class.}^2) \tag{2.14}$$

where

$$R_{class.}^2 = R_0^2 \left(1 - \frac{1}{(2R_0 P_0)^2} \right). \tag{2.15}$$

III. NUMERICAL RESULTS

In the case of an arbitrary mass the integrations must be done numerically. The correlation function shows different behaviour depending on the values of the mass and source parameters. The results of numerical evaluation of eqn.(2.4) are illustrated in figures (3,4). The typical momentum is set to the value

$$P_0 = 1 \ \text{GeV}, \tag{3.1}$$

in order to be comparable with the observed pion spectrum at the Z peak. This implies $R_0 > 0.1$ fm which is consistent with all current estimates of the source size from BE Correlations.

Figure 3 shows the computed correlation function for a source of size 0.2 fm, and for three values of the mass roughly corresponding to the pion, kaon and Λ baryon[1] masses. This corresponds to near the limit of the uncertainty principle ($R_0P_0 = \frac{1}{2}$). As implied in eq(2.12) the correlation is more strongly suppressed in the region $Q > m$ if R_0P_0 is large. This is, in fact, quite general and the opposite is true; when R_0P_0 is close to the uncertainty limit the correlation function is only weakly suppressed. This is because when $R_0^{-1} \sim P_0$, the enhanced region extends over *all* the populated phase space (see discussion and figures from previous section) and averaging over the phase space causes no dilution.

The opposite limit (R_0P_0 large) is explored in figure 4. Here the source radius is $R_0 = 0.8$ fm which takes R_0P_0 sufficiently far from the Heisenberg limit to give strong suppression. The effect is particularly noticeable for the pion correlation which becomes suppressed by a roughly a factor of $4 \sim R_0P_0$ in the region $Q > m$. This leads to typically non-Gaussian shapes for the pion (and other low mass) correlation functions. The suppression differentiates between the kaon and Λ correlations leading to a hierarchy of effective radii, $R_\pi > R_K > R_\Lambda$.

From figures (3,4) one can see that smaller masses give characteristically sharper correlation functions as compared to heavier bosons. One can define an effective radius for the source (somewhat arbitrarily) in terms of the width at e^{-1} of the maximum of the correlation function. This results in the estimates shown in table 1 (see [11] and [12] for pion and kaon measurements respectively).

The reader may wonder if perhaps some intermediate source radius would provide a fit to the experimental radii. This is not the case. If one insists on fitting the source size measured by Λ correlations one is forced to a source of no larger than ~ 0.2 fm. The constraint that $P_0 \sim 1.0$ GeV now leaves R_0P_0 too small to provide the suppression necessary to fit the kaon and pion HBT radii. On the other hand, a source with $R_0P_0 > 1$ leads to natural radii for pion and kaon correlations of order $R_\pi \sim m_\pi^{-1}$ and $R_K \sim m_K^{-1}$ which are larger than experimentally observed. An intermediate choice for R_0 leads to distorted correlation functions which are partially suppressed for $Q > m$. These are difficult to parameterise in terms of a single radius.

It is interesting to note that the correlation function for $R_0P_0 \gg 1$ and $m < P_0$ can be rather well approximated by the expression:

$$C(Q) \approx 1 + \exp(-R_{class}^2 Q^2) \left(\frac{y + (1+y^2)\tan^{-1}(y)}{2y(1+y^2)} \right) \left(\frac{1 + \frac{3Q}{4m} + \frac{Q^2}{m^2}}{1 + \frac{Q}{m}} \right), \tag{3.2}$$

where

$$y = \frac{QR_0P_0}{m}. \tag{3.3}$$

The suppression term multiplying the Gaussian tends to unity as $Q \to 0$, and approaches the value $\frac{\pi m}{2\xi Q}$ as $Q \to \infty$, where $\xi = 2R_0P_0$ as given in eqn.(2.12).

---

[1]Here I plot positive correlations for the antisymmetric $\Lambda\Lambda$ spin state for ease of comparision. The Λ is, of course, a fermion and after spin averaging displays anticorrelations, which lead to a suppression at small relative Q. This does not affect discussion of the HBT radius

IV. CONCLUSIONS

I have shown that the averaging over phase-space to produce a correlation function of a single variable (Q) induces non-trivial, mass dependent distortions on the correlation function. It has been demonstrated that these distortions are such that correlations between smaller mass bosons are inherently shorter range in Q and lead to larger apparent radii. The effect is greatest away from the Heisenberg limit.

For the physically reasonable value of $P_0 = 1.0$ GeV, it is not possible to find a source radius R_0 such that the kinematic averaging simultaneously fits the experimentally measured HBT radii in pion, kaon and Λ baryon correlations. As can be seen from table 1, away from $R_0 P_0 \sim 1$, averaging over phase-space can induce a mass dependence of the HBT radii of the same order of magnitude as experimentally observed (but not with the same absolute values).

Other effects are therefore necessary to bring theory into line with experimental data, but the effects of phase-space averaging should not be neglected.

ACKNOWLEDGMENTS

I am grateful to Ulrich Heinz for many valuable discussions. The hospitality of the CERN Theory Division during this work is gratefully acknowledged. Research supported in part by the EU Programme 'Training and Mobility of Researchers', Network 'Quantum Chromodynamics and the Deep Structure of Elementary Particles', contract FMRX-CT98-0194 (DG 12 - MIHT).

REFERENCES

[1] Z. Kunszt et al, Determination of the Mass of the W Boson, in CERN Yellow Report CERN-96-01, p141-205

[2] A. Ballestrero et al, Report of the Working Group on 'W Mass and QCD' (Phenomenology Workshop on LEP-2 Physics, Oxford, April 1997), J. Phys. G: Nucl.Part.Phys **24** (1998) 365

[3] L. Lonnblad and T Sjostrand, Phys.Lett B**351** (1995) 293

[4] V. Kartvelishvili, R. Kvatadze and R. Moller, Phys. Lett. B**408** (1997) 331

[5] NA49 Collaboration, Nucl. Phys. A**610** (1996) 248c
NA49 Collaboration 'HBT Correlations in 158-A/GeV Pb+Pb collisions', Eur. Phys. J. C**2** (1998) 661

[6] NA35 Collaboration, Nucl. Phys. A**525** (1991) 327c

[7] U. Wiedemann and U. Heinz, Phys. Rept. **319** (1999)
U. Heinz, Nucl. Phys. A**610** (1996) 264c

[8] R. Hanbury-Brown and R.Q. Twiss,Nature **178** (1956) 1046.

[9] A. Bialas and K. Zalewski, Acta. Phys. Pol. B**30** (1999) 359

[10] E. Shuryak, Phys. Lett. B**44** (1973) 387; Sov. J. Nucl. Phys. **18** (1974) 667.

[11] ALEPH Collaboration, Z. Phys. C**54** (1992) 75
DELPHI Collaboration, Phys. Lett B**286** (1992) 201
OPAL Collaboration, Z. Phys, C**72** (1996) 389.

[12] OPAL Collaboration, CERN-EP/99-163
ALEPH Collaboration, Z. Phys C**64** (1994) 361.
DELPHI Collaboration, Phys. Lett. B**379** (1996) 330.
OPAL Collaboration, Z. Phys C**67** (1995) 389.

TABLES

TABLE I. Comparison of the radius parameters extracted from the simple Gaussian model (for $P_0 = 1$ GeV, $R_0 = 0.2$ fm and $R_0 = 0.8$ fm) and experimentally measured values.

Mass / GeV	0.14	0.5	1.1
(Source with $R_0 = 0.2$ fm) Radius / fm	0.32	0.29	0.22
(source with $R_0 = 0.8$ fm) Radius / fm	2.8	1.2	0.9
Experimental Radius / fm	0.9	0.6	0.2

FIGURES

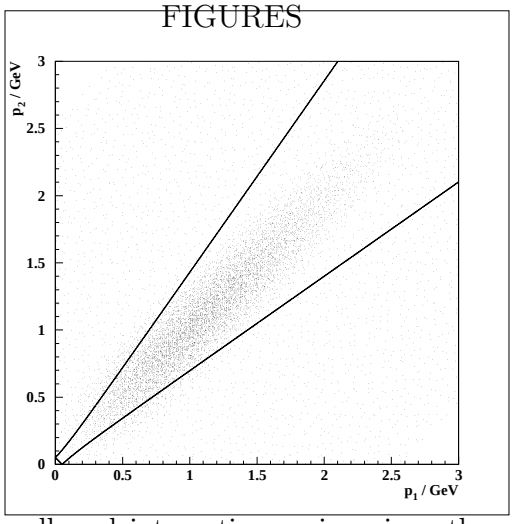

FIG. 1. A plot showing the allowed integration region given the parameters $m = 0.14$ GeV, $Q = 0.05$ GeV, $R_0 = 0.8$ fm and $P_0 = 1.0$ GeV. The scatter shows schematically the enhanced part of the phasespace. For $Q < m$ the integration is mainly over the enhanced region

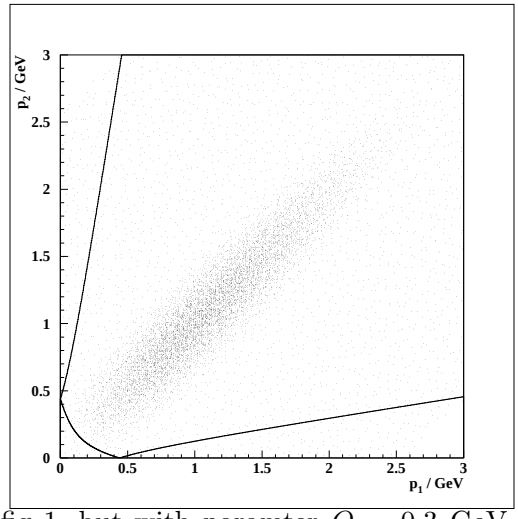

FIG. 2. A similar plot to fig 1, but with paramter $Q = 0.3$ GeV. With $Q > m$ the allowed integration region is not restricted to the enhanced region and the correlation is diluted.

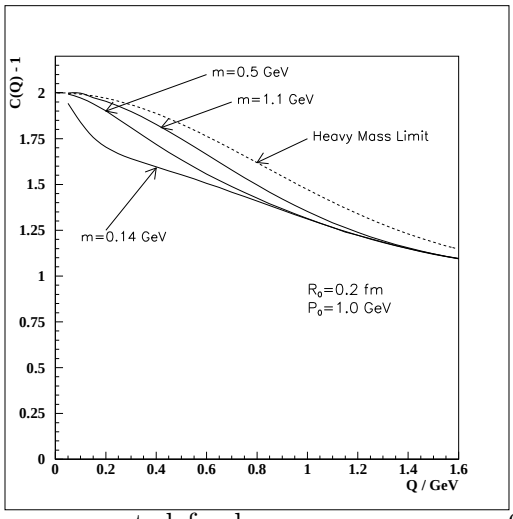

FIG. 3. Correlation functions computed for boson masses $m_\pi \sim 0.14$ GeV, $m_K \sim 0.5$ GeV and $m_\Lambda \sim 1.1$ GeV. The dashed curve shows the correlation function in the extreme heavy mass limit which corresponds to the naive expectation. The correlation functions are computed from a Gaussian source of radius $R_0 = 0.2$ fm and typical momentum $P_0 = 1.0$ GeV, $Q = \sqrt{-(p_1 - p_2)^2}$ - the invariant momentum separation.

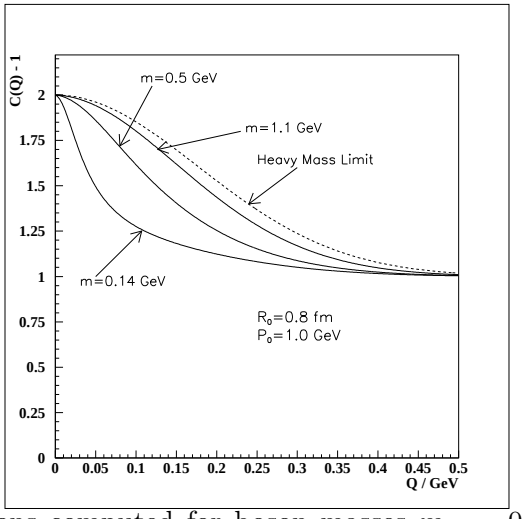

FIG. 4. Correlation functions computed for boson masses $m_\pi \sim 0.14$ GeV, $m_K \sim 0.5$ GeV and $m_\Lambda \sim 1.1$ GeV. The dashed curve shows the correlation function in the extreme heavy mass limit which corresponds to the naive expectation. The correlation functions are computed from a Gaussian source of radius $R_0 = 0.8$ fm and typical momentum $P_0 = 1.0$ GeV, $Q = \sqrt{-(p_1 - p_2)^2}$ - the invariant momentum separation.